Energy 34 (2009) 1315–1324

Contents lists available at ScienceDirect

Energy

journal homepage: www.elsevier.com/locate/energy

Preliminary design and controlling strategies of a small-scale wood waste Rankine Cycle (RC) with a reciprocating steam engine (SE)

M. Badami*, M. Mura

Dipartimento di Energetica, Politecnico di Torino, Corso Duca degli Abruzzi 24, Torino 10129, Italy

ARTICLE INFO

Article history:
Received 27 October 2008
Received in revised form
23 April 2009
Accepted 25 April 2009
Available online 17 June 2009

Keywords:
Biomass
Boiler
Cogeneration
Distributed generation
Expander
Controlling strategies
Rankine Cycle
Reciprocating engine
Renewable energy source
Small-scale CHP
Steam engine
Wood waste

ABSTRACT

In this paper, a small-scale Rankine Cycle (RC) operating as a combined heat and power (CHP) unit and fed by wood waste is studied and the preliminary design and theoretical analysis of the main RC components are presented. A reciprocating single-stage expansion steam engine (SE) was chosen as the expander device: its main characteristics and operative performance are discussed in detail. Finally, the off-design performance is studied with different part-load controlling strategies.

1. Introduction

In the current energy and environmental panorama, where an increase in fossil fuel consumption and in CO_2 production can be observed, the solution to energy and environmental problems is not a simple task since it depends not only on technical factors but also on social and political ones. On the technical side, there are essentially two ways of contributing to energy saving: finding new technologies for efficient energy production or improving the efficiency of the existent technologies, especially those which permit renewable energy sources to be exploited or heat and power to be produced in a distributed way, in particular at a small or medium scale.

Organic Rankine Cycles (ORCs) have recently been developed for use in medium scale CHP systems ($P_{el} > 500$ kW), but some drawbacks of this technology are still evident mainly from the cost point of view and concerning the operation and maintenance of the plant.

Small-scale Steam Rankine Cycles (RCs) were studied in the 70s and 80s for track and vehicle applications and several researchers have demonstrated the feasibility of these systems in relation to the added costs that such systems can involve.

ORCs offer a good solution at the expense of high fluid flow rates and large condenser size. Water Steam Cycles instead, offer higher pressure ratios, which can be obtained with modern heat exchangers and quite small condensers. Water heat-transfer characteristics are better than those of organic fluids. If the shortcomings of water such as freezing and air infiltration could be completely overcome, this would make water the most practical working medium for thermal recovery cycles [1].

The use of small-scale Water Steam RCs that are characterised by a small steam flow rate, shifts the expander technology from turbomachines towards volumetric machines [2], since some of the major problems of using turbines as expanders in small-scale RCs are their very low efficiency, high production costs, especially for multistage turbines, and the possibility of a rapid erosion of the

* Corresponding author. Tel.: +39 011 564.4516; fax: +39 011 564.4599.
E-mail address: marco.badami@polito.it (M. Badami).

0360-5442/$ – see front matter © 2009 Elsevier Ltd. All rights reserved.
doi:10.1016/j.energy.2009.04.031

Nomenclature and acronyms

Nomenclature

c_p	specific heat
h	specific enthalpy
h_c	heat-transfer coefficient
h_{LV}	latent heat
L_c	SE work-per-mass
$\dot{m}_b$	fuel mass flow rate
$\dot{m}_{\text{steam}}$	steam mass flow rate
$\dot{m}_u$	heat user working fluid flow rate
n	rotational shaft speed
P_{aux}	power absorbed by the auxiliaries
P_{el}	net electrical power RC
P_f	power lost due to mechanical friction
P_i	SE internal power
P_{id}	RC ideal power
P_m	SE mechanical shaft power
P_p	electrical power to the RC pump
$\dot{Q}_{\text{steam}}$	heat supplied to steam
$\dot{Q}_{th}$	thermal output
V	displacement
w	fuel moisture (wet basis)
φ	cut-off
ε	compression ratio
$\varepsilon_{\text{boiler}}$	Boiler efficiency
ΔT	temperature difference
η_{ec}	efficiency of the electrical conversion (AC/DC–DC/AC converter)
η_{eg}	efficiency of the electrical generator
	$\eta_{el} = P_{el}/\dot{m}_b \cdot LHV_{\text{wet}}$ electrical efficiency of the RC
η_{id}	RC ideal efficiency
η_{is}	SE isentropic efficiency
η_m	SE mechanical efficiency
	$\eta_{th} = \dot{Q}_{th}/\dot{m}_b \cdot LHV_{\text{wet}}$ thermal efficiency of the RC

Acronyms

CHP	combined heat and power
EUF	$= \eta_{el} + \eta_{th}$ energy utilisation factor
HHV	higher heating value
LHV	lower heating value
ORC	organic rankine cycle
RC	rankine cycle
SE	steam engine
VVA	variable valve actuation
UPS	uninterruptible power supply

turbine's blades due to the moisture content in the expanding steam [3].

Available options of volumetric expanders include reciprocating and rotary expanders, but this last solution, which is often based on the Wankel concept [2,4], shows implementation difficulties [1], while reciprocating SEs result in an easier design and construction [5].

In the light of all these considerations, the authors believe that Water Steam RCs could be reconsidered as one of the best alternatives, in particular as a bottoming cycle in combined cycles [6] or as a power plant technology for wood waste or biomass combustion in a small and compact CHP plant configuration, above all to supply power and heat to remote areas with minimal technical infrastructures.

The design of a small-scale (about 25 kWe) RC operated with a biomass or wood waste Boiler is presented in this paper. The chosen expander technology is a reciprocating single-stage SE with a two cylinder in-line architecture. The SE is fed with superheated steam in order to avoid, or reduce, the formation of condensation during steam admission and expansion.

The activity here presented has been inspired by some of the results obtained in the HEGEL "High Efficiency polyGEneration appLications" project (Contract TREN/05/FP6EN/S07.56687/020153), a European project of the Sixth Framework Programme, coordinated by FIAT Centre of Research, in which three different micro CHP plants have been developed and built, and where a small RC has to be used as bottoming cycle in a combined cycle.

2. Description of the RC system

The small-scale RC cogeneration system presented and studied in this paper is shown in Fig. 1.

Biomass or wood waste is fed to the boiler, where steam, ash and exhaust gas are produced through a combustion process.

Steam is expanded in a single-stage reciprocating engine which is connected to an asynchronous electrical generator to convert mechanical to electrical power. An electronic power unit, composed of one AC/DC and one DC/AC converter, allows the SE to operate at a variable speed, while delivering 50/60 Hz AC to the grid or directly to the electric user. The steam flowing out of the engine is condensed and water is pumped back into the boiler by the feed-water pump. Condensation heat can be used for thermal use (district heating).

The preliminary parameters used for the design of the cogeneration system are reported in Table 1.

The mechanical power, P_m, supplied by the expander can generally be defined as follows:

$$P_m = \eta_m \cdot \eta_{id} \cdot \eta_{is} \cdot \varepsilon_{\text{boiler}} \cdot \dot{m}_b \cdot LHV_{\text{wet}} \tag{1}$$

where η_{id} is the efficiency of the ideal RC, that according with Fig. 2 can be expressed as follows:

$$\eta_{id} = \frac{\left(h_e - h_f\right) - \left(h_b - h_a\right)}{h_e - h_b} \approx \frac{\left(h_e - h_f\right)}{h_e - h_b} \tag{2}$$

and that, considering the thermodynamic parameters of the system at the rated condition, (see Table 1), assumes a value of 0.325.

In Fig. 3 the behaviour of the RC ideal efficiency as a function of the maximum pressure, maximum temperature and back pressure

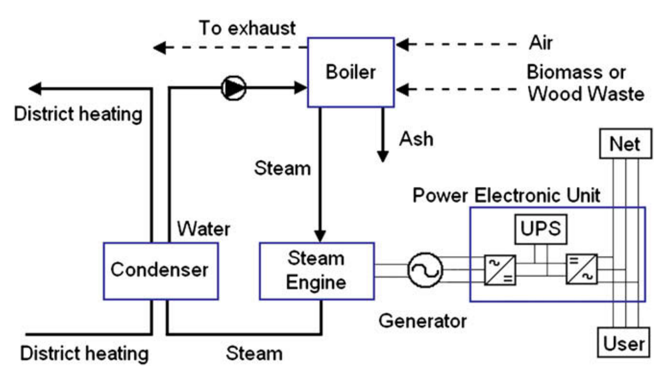

Fig. 1. RC fed with biomass or wood waste.

Table 1
Preliminary parameters of the system at the rated condition.

Parameter	Value
Fuel Input ($\dot{m}_b \cdot LHV_{\text{wet}}$)	162 kW
Steam superheated temperature	450 °C
Steam superheated pressure	100 bar
Condensation pressure	1 bar, ($T_{sat} \approx 100$ °C)

is shown. As it is well known, an increase of the cycle maximum pressure and temperature determines an increase of the RC efficiency. As far as the system analysed in this paper is considered, a maximum pressure of 100 bar and a temperature of 450 °C were chosen: these values represent a good compromise between high efficiency and technical limits of standard technologies. A condensation pressure/temperature of 1 bar/100 °C respectively was chosen in order to produce hot water for district heating.

The net electrical power, P_{el}, supplied by the RC can be calculated as follows:

$$P_{el} = \eta_{ec} \cdot \eta_{eg} \cdot P_m - P_p \tag{3}$$

where η_{ec} is the efficiency of the electrical conversion (AC/DC–DC/AC converter), η_{eg} is the efficiency of the electrical generator and P_p is the electrical power to the RC pump.

Finally, the heat supplied to the thermal user, $\dot{Q}_{th}$, can be defined as:

$$\dot{Q}_{th} = \dot{m}_u \cdot c_{p,u} \cdot \Delta T_u \tag{4}$$

where $\dot{m}_u$ is the flow rate of the working fluid used by the thermal user and ΔT_u is the temperature difference between the inlet and outlet working fluid of the thermal user.

3. Biomass boiler

As far as the boiler type is concerned, an once through biomass boiler [7] is considered in this work (see Fig. 4 for a general scheme). This boiler besides the traditional sub-systems (such as fuel handling/drying/combustion zones, feed-water treatment, air and water delivery and control, emissions reduction, ash handling) is supposed to be equipped with a steam generator similar to the capillary once through steam generator that now is under development in a heat recovery asset for the European HEGEL project [6].

Boiler performance depends on several parameters such as boiler design (e.g. down-draught combustion or up-draught combustion), fuel used, flow rate of the fuel and air, combustion rate, excess air, etc.

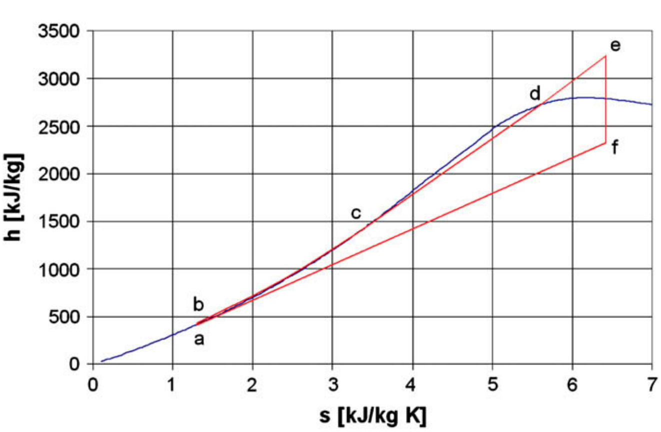

Fig. 2. Mollier diagram of the ideal RC.

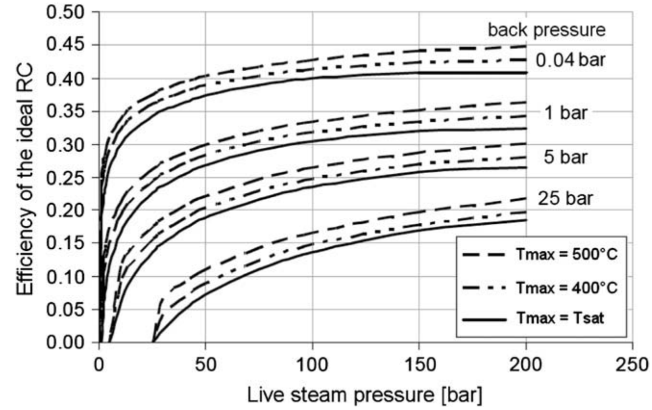

Fig. 3. Influence of maximum pressure, maximum temperature and back pressure on the efficiency of an ideal RC.

Boiler losses can be significant and schematically include [8]:

1. heat carried away by the flue gases (dry products of combustion), including CO_2, CO, N_2, O_2, etc.;
2. heat needed to heat and evaporate the water content in the fuel and air;
3. heat taken away by the wet combustion product;
4. radiation and convection losses;
5. energy loss due to incomplete combustion and energy loss to the ash.

The first three types of losses are the most important: they purely depend on the fuel and air moisture contents and on the amount of excess air used in the combustion, which is defined as the ratio between the real flow rate of air involved in the combustion with the stoichiometric air flow rate. The fourth and fifth losses can be minimized through a good design of the combustion chamber and an accurate control of the combustion temperature.

In this paper wood with an average composition, like that presented in Table 2, was taken into account in the subsequent calculations.

The energy content of the fuel (dry basis) was assessed using the following correlation suggested by [9] as a best fit correlation (absolute error less than 2.59%):

$$HHV_{\text{dry}} = -1.3675 + 0.3137 \times C + 0.7009 \times H + 0.0318 \times O^a \tag{5}$$

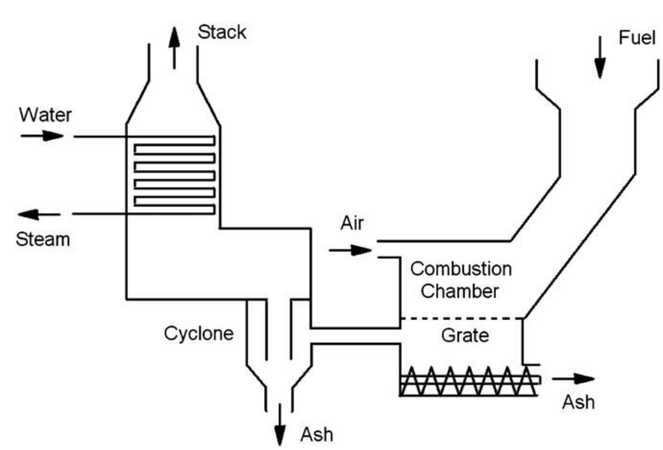

Fig. 4. Schematic diagram of a wood-fired boiler system.

Table 2
Fuel composition considered.

Fuel composition	
Ultimate analysis (dry basis)	
C	46%
H	7%
O	44%
S	1%
HHV_{dry} of eq. (5)	19.4 MJ/kg
Proximate analysis	
Ash	2% (dry basis)
Fuel moisture (w)	33% (wet basis)
LHV_{wet}	11.6 MJ/kg

where the fuel composition (C, H, O^a) is the weight percent of the dry biomass, and where O^a is the sum of the oxygen contents and other elements in the organic dry matter. LHV_{dry} was calculated from HHV_{dry} subtracting the latent heat (h_{LV}) at ambient pressure of water produced by the combustion.

The minimum amount of air required for a complete combustion of the fuel can be easily determined from the chemical composition and from the moisture content in the fuel. In practise, the stoichiometric amount of air is not sufficient to ensure complete combustion, since the solid fuel cannot all be in close contact with oxygen. In order to maximize the degree of combustion completeness, extra air is introduced into the furnace. In the calculations presented in this paper, excess air equal to 50% [7] was considered.

In order to study the boiler behaviour and performance, a simulation with Gate-Cycle™ software was carried out; this analysis made it possible to determine the flow rate of generated steam and the exhaust gas temperature at the exit of the boiler, for the fuel in Table 2.

The steam flow rate and flue gas temperature are reported in Fig. 5 as a function of the fuel input; at the maximum fuel flow rate in input (162 kW), the boiler burns about 50 kg/h of wood and the exhaust gas temperature is approximately 200 °C.

The boiler efficiency was calculated by means of the following equation:

$$\varepsilon_{boiler} = \frac{\dot{Q}_{steam}}{\dot{m}_b \cdot LHV_{wet}} = \frac{\dot{m}_{steam} \cdot (h_e - h_b)}{\dot{m}_b \cdot LHV_{wet}} \tag{6}$$

The boiler efficiency is shown as a function of the fuel heat flow rate in Fig. 6.

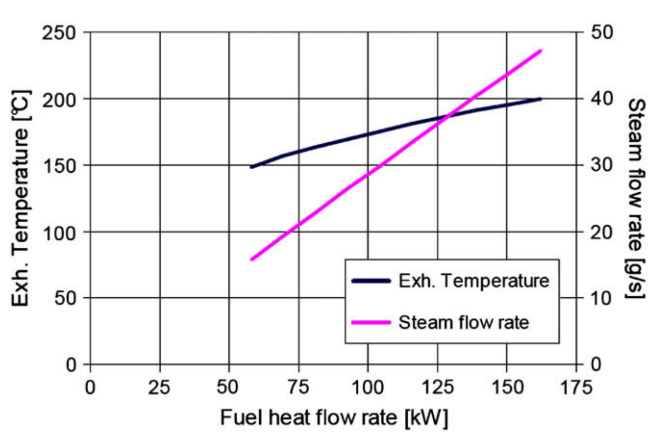

Fig. 5. Boiler steam flow rate and flue gas temperature as a function of the fuel heat flow rate from wood waste.

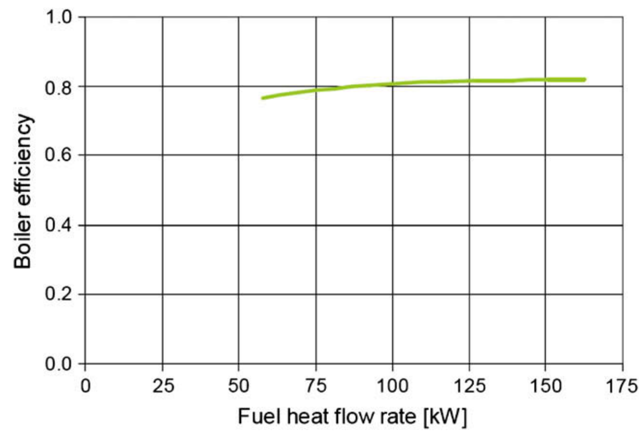

Fig. 6. Boiler efficiency as a function of the fuel heat flow rate.

4. Steam engine

The RC expander considered in this work is a reciprocating single-stage single-acting SE with a two in-line cylinder architecture. The single-acting single-expansion solution was chosen because it simplifies the engine architecture and the valve distribution system at the expense of a lower power density.

A brief description of SE technology is given in this section, which shows the most important performance parameters that can be used for a complete characterization of this device. The best sizing of the SE is discussed at the end of the paragraph.

4.1. SE theory

Fig. 7 shows the ideal working cycle of the SE, which consists of the following phases:

- Compression stroke (1 → 2): in this phase (from Bottom Dead Centre to Top Dead Centre), the residual steam is compressed in the cylinder.
- Admission (2 → 3) and (3 → 4): steam at high pressure is forced into the cylinder through the intake port.

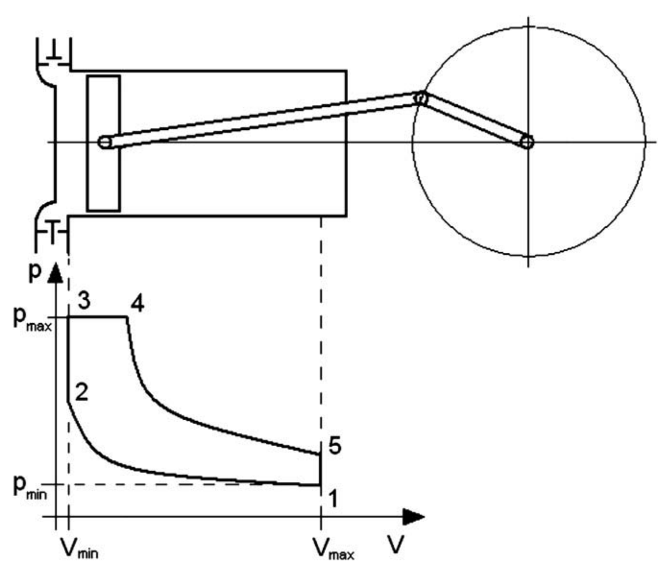

Fig. 7. Ideal cycle for a reciprocating SE.

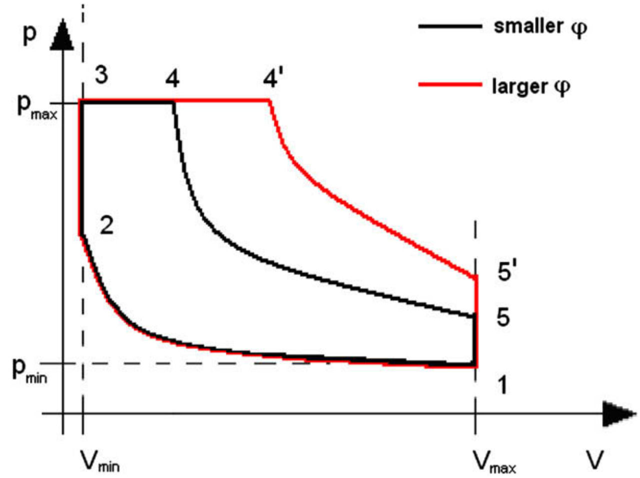

Fig. 8. Influence of cut-off on the ideal working cycle.

- Expansion (4 → 5): the steam at high pressure pushes the piston towards the BDC; this phase, along with (3 → 4), is also called power stroke.
- Exhaust (5 → 1): the steam flows out of the engine, and the pressure is thus reduced to the thermodynamic conditions in the condenser.

In the ideal working cycle, two losses are evident:

- The expansion stoke is incomplete; at point 5 steam flows out of the cylinders from the outlet valve at high pressure with a waste of working energy.
- In the first part of the admission phase (2 → 3), the incoming steam compresses the steam contained in the dead volume, without producing work.

The work-per-cycle and the isentropic efficiency are defined as follows:

$$L_c = \oint p dV \quad [\mathrm{J/cycle}] \tag{7}$$

$$\eta_{is} = \frac{P_i}{P_{id}} = \frac{n \cdot i \cdot L_c}{\dot{m}_{\mathrm{steam}} \cdot \left(h_e - h_f\right)} \tag{8}$$

where P_i is the internal power, n is the speed of the engine and i is the number of cylinders.

For the ideal cycle in Fig. 7, it is easy to develop an analytic expression for (7) and (8), as is shown in (9) and (10).

$$L_c = p_{\max} \cdot V \cdot \left\{ \varphi + \frac{1 + \varphi \cdot (\varepsilon - 1)}{(k-1) \cdot (\varepsilon - 1)} \cdot \left[1 - \left(\frac{1 + \varphi \cdot (\varepsilon - 1)}{\varepsilon} \right)^{k-1} \right] \right\} - p_{\min} \cdot V \cdot \frac{\varepsilon \cdot \left(\varepsilon^{k-1} - 1 \right)}{(k-1) \cdot (\varepsilon - 1)} \tag{9}$$

$$\eta_{is} = \frac{p_{\max} \cdot \left\{ \varphi + \frac{1+\varphi \cdot (\varepsilon-1)}{(k-1) \cdot (\varepsilon-1)} \cdot \left[1 - \left(\frac{1+\varphi \cdot (\varepsilon-1)}{\varepsilon} \right)^{k-1} \right] \right\}}{\frac{h_e - h_f}{\varepsilon - 1} \cdot \left[\frac{1 + \varphi \cdot (\varepsilon - 1)}{v_5} - \frac{\varepsilon}{v_2} \right]} - \frac{p_{\min} \cdot \left[\frac{\varepsilon \cdot \left(\varepsilon^{k-1} - 1 \right)}{(k-1) \cdot (\varepsilon - 1)} \right]}{\frac{h_e - h_f}{\varepsilon - 1} \cdot \left[\frac{1 + \varphi \cdot (\varepsilon - 1)}{v_5} - \frac{\varepsilon}{v_2} \right]} \tag{10}$$

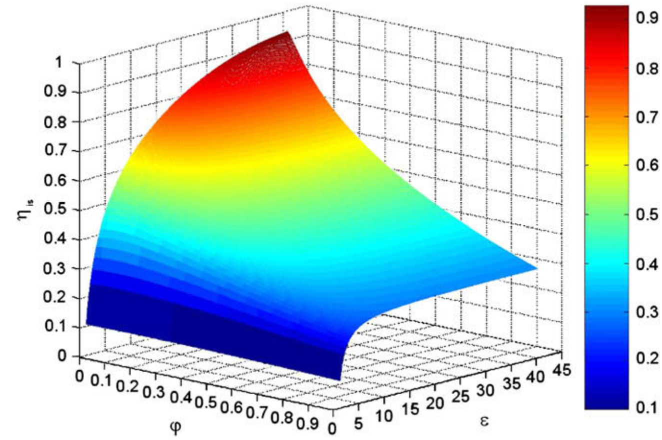

Fig. 9. Isentropic efficiency of the SE as a function of ε and φ for the analysed thermodynamic conditions of RC.

From this analysis it is clear that the ideal efficiency and the work-per-cycle, which is the area in the p_V graph of the ideal cycle, depend on the thermodynamic conditions of the steam in admission and in the condenser, and on two parameters: the compression ratio ε and the steam cut-off timing φ [10–13], which are defined as follows:

$$\varepsilon = \frac{V_{\max}}{V_{\min}} = \frac{V}{V_{\min}} + 1 \tag{11}$$

$$\varphi = \frac{V_4 - V_{\min}}{V_{\max} - V_{\min}} = \frac{V_4 - V_{\min}}{V} \tag{12}$$

While the ratio condition ε is a geometrical parameter defined by the internal geometry of the engine, the cut-off timing φ is an operating parameter, which depends basically on timing of closing inlet valve, and is almost directly proportional to the amount of the working steam per cycle. The ideal working cycle results to be thinner for a small cut-off (see Fig. 8) and produces smaller torque but higher ideal efficiency (see Figs. 9 and 10). The ideal working cycle for high cut-off values instead results to be larger (see Fig. 8) and produces higher torque but lower ideal efficiency (see Figs. 9 and 10).

The influence of ε on the isentropic efficiency can clearly be observed in Fig. 10: high compression ratio values allow the efficiency to be improved, whatever φ value is used; a value of 30 for ε could be reached using of poppet valves and a specific design of the piston and head of the SE. This value has been used for the mechanical design of the engine.

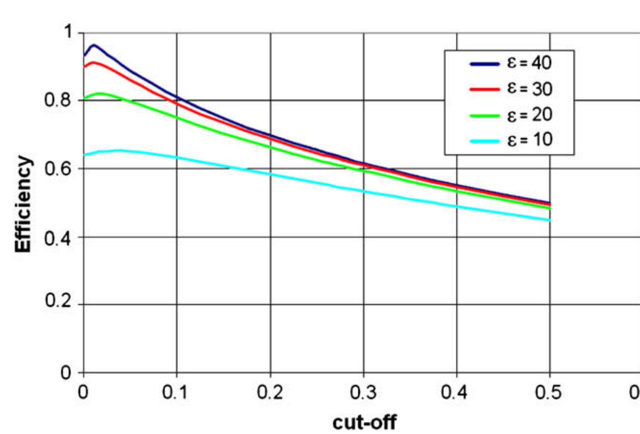

Fig. 10. Isentropic efficiency of the SE as a function of φ for several values of ε for an ideal cycle.

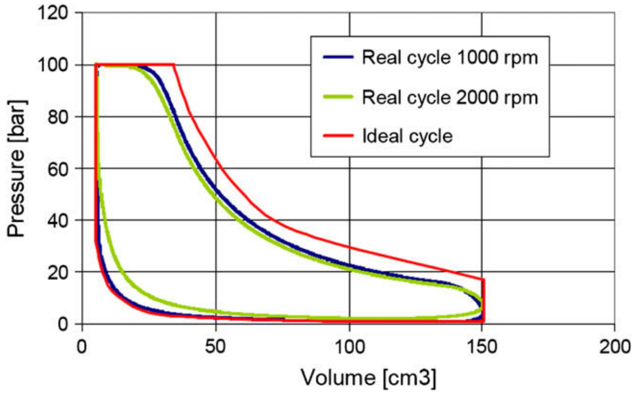

Fig. 11. Comparison between real and ideal cycles at constant cut-off.

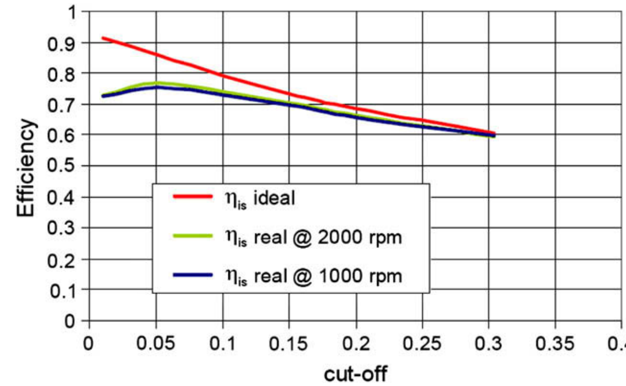

Fig. 12. Comparison between ideal cycle isentropic efficiency versus cut-off ($\varepsilon = 30$) and isentropic efficiency of two real cycles at 2000 rpm and 1000 rpm.

Passing from the ideal to the real working cycle, other causes of irreversibility should be considered. In particular, the following differences between ideal and real work cycles are evident [10–14]:

- Dissipative effects of a fluid-dynamic nature in steam admission and exhaust from the cylinders.
- Admission, expansion, exhaust and compression strokes are not adiabatic processes and heat exchanges should be taken into account between the working fluid and the internal walls of the SE.
- Steam leaks which determine work losses should be considered.

The isentropic efficiency given in (8) was then calculated for a modelled real cycle which takes into account all the main losses above mentioned.

As far as the dissipative fluid-dynamic effect on the steam is concerned, a detailed valve model, which takes into account consideration typical experimental flow coefficients, was used to simulate the flow through inlet and exhaust valves. To simulate the effects of the heat exchange, a model which takes into account the influence of the speed has been considered. In particular, a loss equal to 5% of the work-per-cycle [14] has been considered at $n = 2000$ rpm and the influence of the speed has been taken into account, considering that the heat-transfer coefficient is proportional to the speed of the engine ($h_c = \text{constant} \times n^{0.8}$) [15] while the heat exchange time per cycle is equal to $1/n$. As far as leakages are concerned, the lost mass per cycle has been calculated to be equal to 2% of the mass expanded per cycle for $n = 2000$ rpm, while its variation with regard to the speed of the engine was considered to be proportional to $1/n$.

In Fig. 11 an ideal cycle with cut-off $\varphi = 0.2$ and compression ratio $\varepsilon = 30$ is compared to two modelled "real" cycles at 1000 rpm and at 2000 rpm with the same cut-off and compression ratio. The outcome of dissipative effects, of heat exchanges and of leakages is evident in the figure.

The comparison between the isentropic efficiency of the ideal work cycle and the real work cycles versus cut-off is shown in Fig. 12; in this figure $\varepsilon = 30$ and the real cycles are calculated at 2000 rpm and 1000 rpm.

In order to calculate the mechanical power supplied to the shaft of the engine, the mechanical losses and the power necessary to activate the auxiliaries must be considered. η_m can be determined using the following equation:

$$\eta_m = \frac{P_m}{P_i} = \frac{P_i - \left(P_f + P_{\text{aux}}\right)}{P_i} \tag{13}$$

where P_f is the power loss due to mechanical friction and P_{aux} is the power absorbed by the auxiliaries (e.g. pumps, valve actuation system, etc…). In [10], the mechanical efficiency for SEs was estimated to span from 85% to 95%. In this present paper, the authors have considered a mechanical efficiency at rated conditions equal to 90%. In order to determine the behaviour of the mechanical efficiency at part-load conditions, the Chen–Flynn model [16], originally suggested for a compression ignition engine, was considered. The soundness of this assumption can be inferred from the fact that the two engines (compression ignition engine and SE) have a similar architecture and lubrication system [17]. The influence of this assumption is discussed in the Sensitivity and Error Analysis section. The mechanical efficiency behaviour can be represented as a function of the cut-off by means of the Chen–Flynn model, as is shown in Fig. 13. The isentropic efficiency and the product of the mechanical and isentropic efficiencies are also reported in the same figure.

4.2. SE sizing

The optimal size of the SE should be obtained satisfying three different needs:

a) the SE has to operate with as high an efficiency as possible;
b) the SE must be able to expand the entire steam flow rate generated by the boiler;
c) the SE must be as compact as possible (low displacement).

The behaviour of the product between isentropic and mechanical efficiency is shown in Fig. 13; it is possible to see that the maximum efficiency (>0.6) is obtained in a range of cut-off between 0.06 and 0.26.

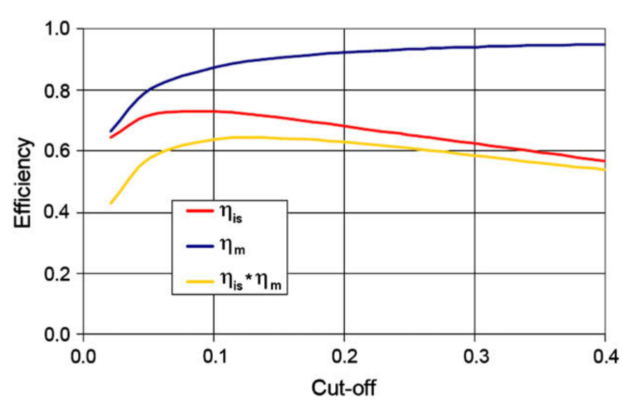

Fig. 13. Efficiencies of the SE as a function of cut-off ($n = 2000$ rpm).

Table 3
Technical features of the SE.

Steam engine	
Configuration	2 cylinders in line
Bore/Stroke	57/57 mm
Displacement	295 cm^3
Number of valves per cylinder	2
Nominal speed	2000 rpm
Nominal inlet pressure/temperature	100 bar/450 °C
Nominal outlet pressure	1 bar
Nominal steam flow rate	47 g/s
Minimum steam flow rate	16 g/s

In order to meet the third need (compactness of the engine), it was then decided not to use the value of the cut-off corresponding to the maximum efficiency ($\varphi = 0.11$, which corresponds to $\eta_{is} \cdot \eta_m = 0.64$) but a higher value. In particular, a nominal cut-off value equal 0.17 was chosen ($\eta\eta_{is} \cdot \eta_m = 0.63$) and, considering a nominal steam flow rate equal to 47 g/s and a nominal speed of 2000 rpm, a displacement $V = 295$ cm^3 was then derived. It is important to point out that if a cut-off $\varphi = 0.11$ was chosen, for the same nominal flow rate and speed, a displacement of about 450 cm^3 would have been determined, with an evident big increase in the size and weight of the engine.

The main design characteristics of the SE are reported in Table 3.

Two schemes of the main SE components are shown in Figs. 14 and 15.

5. Condenser

The analysed RC is in a back-pressure configuration, so that all the heat generated from steam condensation is destined for the thermal user at a temperature that is established according to the final utilisation (between 85 and 90°).

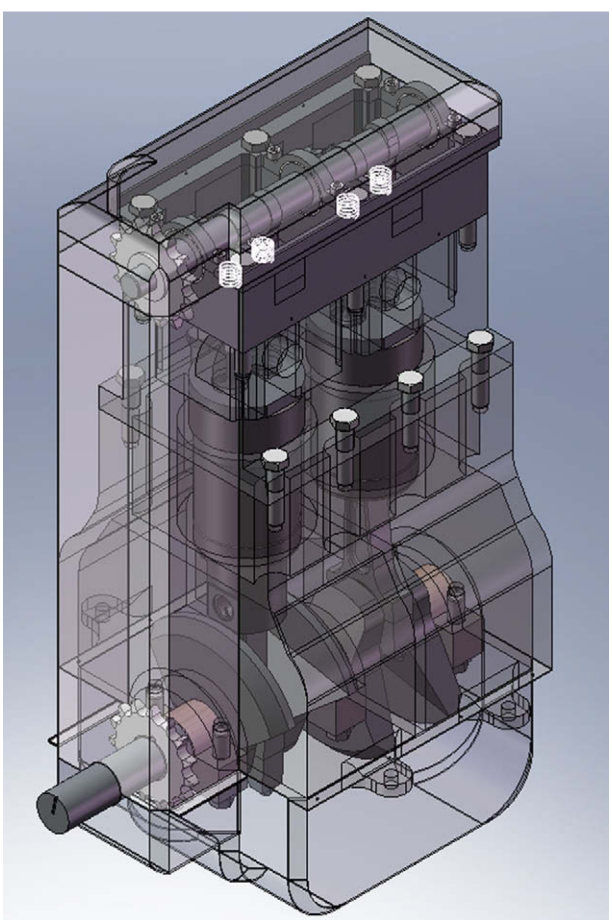

Fig. 14. 3D picture of the sized SE.

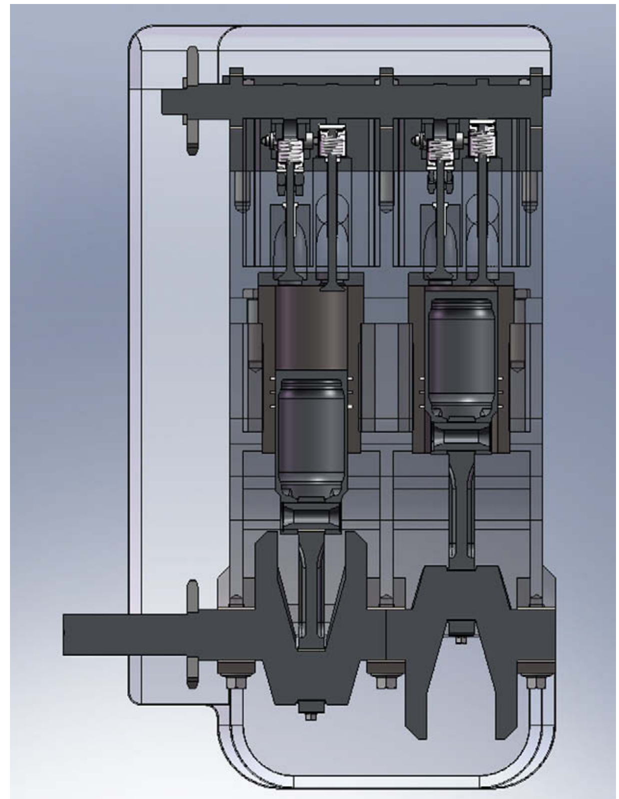

Fig. 15. 3D section of the SE.

The operating condenser conditions and main dimensional characteristics are summarised in Table 4.

6. Power control of the RC

The power control of the RC should obviously be obtained first of all acting on the boiler, while the pressure and temperature at the inlet of the SE can be regulated by controlling the water flow rate from a feed volumetric pump and the steam flow rate expanded by the SE. While the feed pump control can be easily obtained by acting, for example, on the speed of the pump, controlling the SE can be quite difficult. Three different kinds of controlling action can be considered (see Fig. 16):

- Variable speed at constant cut-off (1)
- Variable cut-off at constant speed (2)
- Valve governing (3)

6.1. *Variable speed strategy (1)*

In this case, the steam distribution in the SE is considered to be obtained by means of poppet valves actuated by a traditional

Table 4
Main parameters of the condenser.

Condenser	
Type	Shell and tube
Maximum pressure (safety) [bar]	100
Operating inlet pressure [bar]	1
Operating condensation temperature [°C]	100

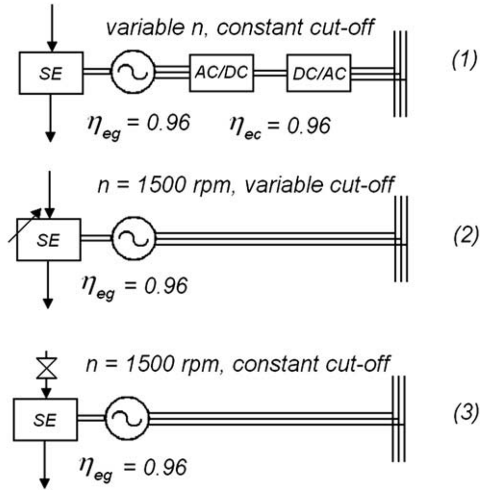

Fig. 16. Schemes of the three considered controlling actions.

camshaft rocker-rod mechanism. The steam flow rate is then adjusted controlling the rotational speed variation.

The speed control is obtained with an electronic power system (AC/DC and DC/AC converter) that allows the engine speed to be changed from 600 rpm to 2000 rpm in order to expand the entire produced steam flow rate.

The operative conditions considered in the following analysis are presented in Table 5.

The net electrical power of the RC as a function of the speed is shown in Fig. 17.

Line (1) in Fig. 19 shows the RC efficiency as a function of the RC electrical power for the variable speed strategy.

6.2. Variable cut-off strategy (2)

In this case, a variable valve actuation (VVA) is used to control the cut-off and thus the steam flow rate and the power of the SE. The speed is constant and assumed equal to 1500 rpm: the electrical generator can be directly connected to the SE (European grid, 50 Hz).

The operative conditions considered in the following analysis are presented in Table 6.

As far as the cut-off actuation is concerned a VVA similar to those used in automotive engines should be considered.

The net electrical power of the RC as a function of the cut-off is shown in Fig. 18.

Line (2) in Fig. 19 shows the electrical efficiency as a function of the RC electrical power for the variable cut-off strategy.

Since the power absorbed by VVA is considered in literature [17] to be comparable with the conventional valvetrain, the same mechanical efficiency model as strategy (1) was considered for strategies (2).

6.3. Governing valve strategy (3)

This kind of controlling strategy is very simple because the SE power reduction is obtained by reducing the steam pressure at the

Table 5
Main parameters for the variable speed strategy.

Variable speed strategy	
Nominal speed	2000 rpm
Cut-off	0.17
η_{eg}	0.96
η_{ec}	0.96

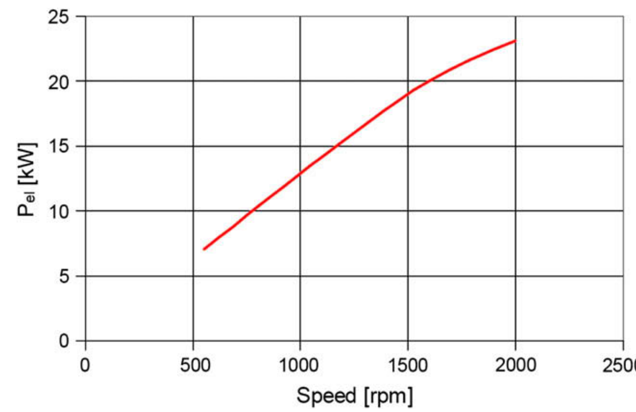

Fig. 17. Net electrical power as a function of speed.

SE inlet using a governing valve. This strategy offers the advantage of operating the SE at constant cut-off and at constant speed but, on the other hand, this kind of controlling action leads to a great reduction of the RC efficiency.

A traditional camshaft and a rocker-rod mechanism with a constant profile of the inlet and exhaust cams can be used with this kind of controlling action.

Since the SE works at constant speed (1500 rpm), it is possible to directly connect the electrical generator to the electrical grid.

The operative conditions considered in this work are presented in Table 7.

The RC efficiency calculated with a governing valve control strategy is shown in line (3) in Fig. 19.

6.4. Comparison of the different strategies

From Fig. 19 it is possible to note that the strategy with the variable cut-off (2) results to be the most efficient on almost the entire controlling range, while the valve governing strategy (3) appears as the most inefficient strategy with the exception of the high part load.

Table 6
Main parameters for the variable cut-off control strategy.

Variable cut-off strategy	
Speed	1500 rpm
Nominal cut-off	0.22
η_{eg}	0.96

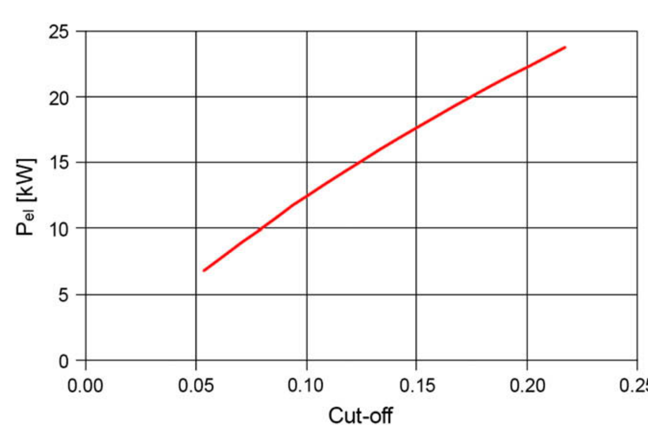

Fig. 18. Net electrical power as a function of cut-off.

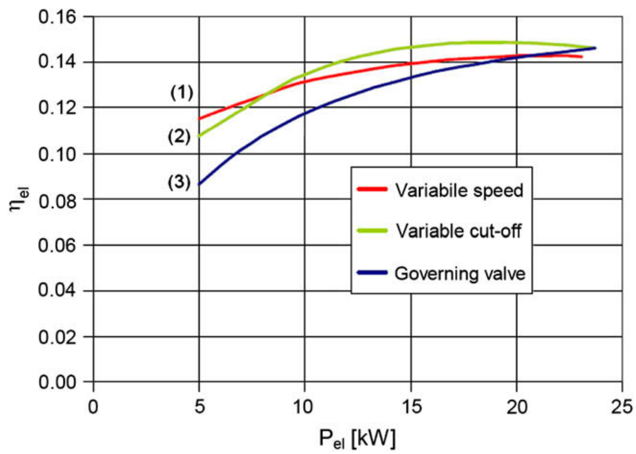

Fig. 19. Comparison of the three part load strategies.

Table 7
Main parameters for the variable cut-off control strategy.

Valve governing strategy	
Speed	1500 rpm
Cut-off	0.22
η_{eg}	0.96

Finally, the variable speed strategy (1) shows an efficiency that falls between the two previous strategies and, due to the recent enhancement of power electronic technology, it can be quite easily put in action. For this reason and because of the previous considerations, the authors consider the variable strategy a good trade-off between efficiency and simplicity of the system.

7. Cogeneration indicators

Considering to use a variable speed strategy for the SE part-load operation, the thermal output to the end user and the EUF have been calculated according to eqs. (3) and (4).

The thermal output is shown in Fig. 20 as a function of the electrical power. As it is possible to see, this parameter is almost directly proportional to the supplied electrical power.

The behaviour of the thermal and the electrical efficiency and the Energy Utilisation Factor (EUF) of the system are shown in Fig. 21. The thermal efficiency, as a function of the electrical power, is almost constant over the entire operating range and it is approximately equal to 64%, while the electrical efficiency shows a constant value of 14%. Since both the electrical efficiency and thermal efficiency have almost constant behaviour in the operating range, the EUF also shows an almost constant value of about 78%.

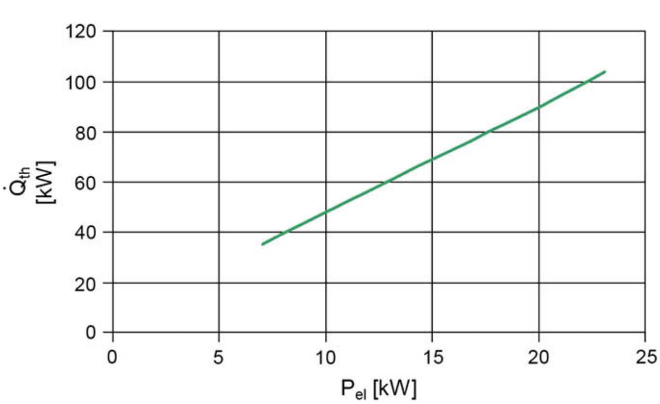

Fig. 20. Thermal output as a function of the electrical power supplied.

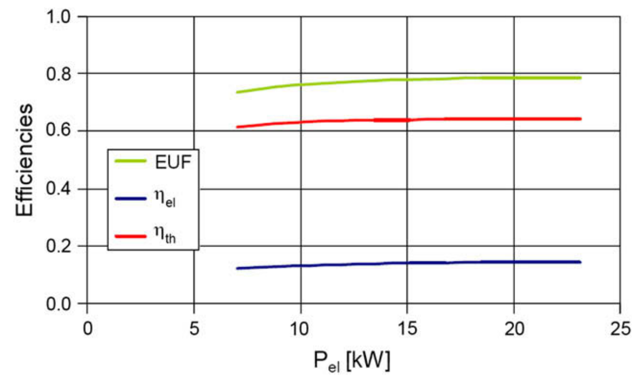

Fig. 21. Cogeneration indicators as a function of the electrical power supplied.

8. Sensitivity analysis

In order to validate the previously presented study, some considerations on the sensitivity of the RC model have been summarised.

The model was obtained performing a traditional analysis of the plant through the well known energy balance and thermodynamic equations. A sensitivity analysis on the electrical power output (P_{el}) of the RC and on electrical efficiency (η_{el}) was carried out under the hypothesis of a relative uncertainty equal to ±2.5% for each parameter. The analysis was conducted on working conditions related to the maximum electrical power supplied (variable speed controlling system).

The electrical power output can be calculated by means of eq. (3) as a function of several parameters:

$$P_{el} = f\left(\eta_{ec} \times \eta_{eg}, \eta_m, \eta_{is}, \eta_{id}, \varepsilon_{\text{boiler}}, \dot{m}_b, LHV_{\text{wet}}, P_p\right) \tag{14}$$

The general law of uncertainty propagation proposed in the ISO "Guide to the Expression of Uncertainty in Measurement" [18] was used to determine the uncertainty of the calculated parameters (P_{el}, η_{el}). The absolute uncertainty U_f associated to a calculated parameter $f(x_i)$, is related to the uncertainties U_i of each parameters x_i by means of the following formula [18]:

$$U_f = \pm\sqrt{\sum_{i=1}^{n}\left(\frac{\partial f}{\partial x_i}\cdot U_i\right)^2}. \tag{15}$$

Table 8
Sensitivity analysis of the RC system.

Parameter	Estimated value	Uncertainty	
		Absolute "U"	Relative (%) "u"
RC sensitivity analysis – independent parameters			
$\eta_{ec} \times \eta_{eg}$	92%	±2.30%	±2.5%
η_m	90%	±2.25%	±2.5%
η_{is}	67.5%	±1.69%	±2.5%
η_{id}	32.5%	±0.81%	±2.5%
$\varepsilon_{\text{boiler}}$	81.5%	±2.04%	±2.5%
$\dot{m}_b$	0.014 kg/s	±0.00035 kg/s	±2.5%
LHV_{wet}	11554 kJ/kg	±228.9 kJ/kg	±2.5%
P_p	0.9 kW	±0.023 kW	±2.5%
RC sensitivity analysis – calculated parameters			
Electrical Power Output (P_{el})	23.1 kW	±1.59 kW	±6.88%
Electrical Efficiency (η_{el})	14.3%	±1.11%	±7.74%

The relative uncertainty can be calculated as follows:

$$u_f = \frac{U_f}{f(x_i)}. \quad (16)$$

The numerical results of the sensitivity analysis on P_{el} and on η_{el}, obtained by means of eqs. (15) and (16), are shown in Table 8.

9. Conclusions

A small-scale steam RC cogeneration unit (electrical power equal to 23 kW, thermal output equal to 104 kW), using wood waste as fuel, has been presented in this paper. The proposed system shows an electrical efficiency of about 14% and an EUF of about 78%; these performances are approximately constant in the working range of interest. The most important peculiarity of the system is that the steam expander is a reciprocating single-expansion SE.

The analysis has in fact shown that the SE could be an interesting technology for small-scale energy plants and offers a good solution when fed with wood waste.

The main losses in the SE have been calculated and discussed in the paper.

The guidelines for a rapid sizing of the expander are presented in the work, showing what criteria should be adopted to obtain a compact SE with good efficiency.

Different controlling strategies have been considered. From an efficiency point of view, the variable cut-off strategy is better than the others, nevertheless, this solution needs a quite difficult technical design and construction. The variable speed strategy is characterised by lower efficiency, but can be more easily obtained using an electronic power system composed of an AC/DC and a DC/AC converter; a traditional camshaft rocker-rod mechanism is used for poppet valve actuation. The last strategy permits the power of the system to be controlled by means of a governing valve; this controlling action is the simplest, but at the same time the worst in terms of efficiency.

For all these reasons, the variable speed strategy has been considered by the authors to be the best solution as regards the trade-off between efficiency and complexity.

Acknowledgments

The support provided by the EU Sixth Framework Programme Priority 6.1 (contract TREN/05/FP6EN/S07.56687/020153, HEGEL Project, “High Efficiency polyGEneration appLications”) is gratefully acknowledged. The authors would also like to express their gratitude to P. Platell (Ranotor, Sweden) and M. Bernas (Energiprojekt AB, Sweden) for their help and advice.

References

[1] Stobart R, Weerasinghe R. Heat recovery and bottoming cycles for SI and CI engines – a perspective. SAE; 2006. 01-0662.
[2] Badr O, Naik S, O’Callaghan PW, Probert SD. Expansion machine for a low power-output steam Rankine-Cycle engine. Applied Energy 1991;39:93–116.
[3] Bahadori MN. Solar water pumping. Solar Energy 1978;21:307–16.
[4] Badr O, O’Callaghan PW, Hussein M, Probert SD. Rotary Wankel Engine as expansion devices in steam Rankine-Cycle engines. Applied Energy 1991;39:59–76.
[5] Bidini G, Manuali A, Saetta S. Reciprocating steam engine power plants fed by wood waste. International Journal of Energy Research 1998;22:237–48.
[6] Badami M, Mura M, Campanile P, Anzioso F. Design and performance evaluation of an innovative small scale combined cycle cogeneration system. Energy 2008;33:1264–76.
[7] Van Loo S, Koppejan J. Handbook of biomass. Combustion and co-firing. Enschede: Twente University Press; 2002.
[8] Prasad SB. Biomass-fired steam power cogeneration system: a theoretical study. Energy Conversion and Management 1995;36:65–77.
[9] Changdong S, Azevedo JLT. Estimating the higher heating value of biomass fuels from basic analysis data. Biomass & Bioenergy 2004;28:499–507.
[10] Brunelli PE. The steam engines (Le macchine a vapore). Ing. In: Giorgio V, editor. Turin; 1946 [in Italian].
[11] Capetti A. Steam engines (Motori a vapore). Ing. In: Giorgio V, editor. Turin; 1953 [in Italian].
[12] Harding LA. Steam power plant engineering. New York: John Wiley & Sons, Inc; 1932.
[13] Stumpt J. The una – flow steam-engine; 1922.
[14] Stokes PR. Piston steam engine innovation. Proceeding of the Institution of Mechanical Engineers, Part A: Journal of Power and Energy 1996;210:95–8.
[15] Heywood JB. Internal combustion engine fundamentals. McGraw-Hill; 1988.
[16] Chen SK, Flynn PF. Development of compression ignition research engine. SAE; 1965. 650733.
[17] Burak G. A low-friction variable-valve-actuation device part I: mechanism description and friction measurements. SAE; 1997. 970338.
[18] ISO/IEC Guide 98:1995. Guide to the expression of uncertainty in measurement (GUM); 1995.